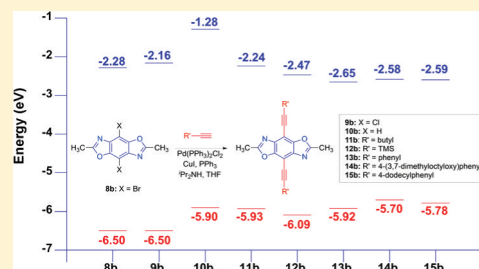


Tuning the Optical and Electronic Properties of 4,8-Disubstituted Benzobisoxazoles via Alkyne Substitution

Brian C. Tlach,[†] Aimée L. Tomlinson,[‡] Achala Bhuwarka,[†] and Malika Jeffries-EL^{*,†}[†]Department of Chemistry, Iowa State University, Ames, Iowa 50010, United States[‡]Department of Chemistry, North Georgia College & State University, Dahlonega, Georgia 30597, United States

Supporting Information

ABSTRACT: In an effort to design new electron-deficient building blocks for the synthesis of conjugated materials, a series of new *trans*-benzobisoxazoles bearing halogen or alkynyl substituents at the 4,8-positions was synthesized. Additionally, the impact of these modifications on the optical and electronic properties was investigated. Theoretical calculations predicted that the incorporation of various alkynes can be used to tune the energy levels and band gaps of these small molecules. The targeted 4,8-disubstituted benzobisoxazoles were easily prepared in good yields using a two-step reaction sequence: Lewis acid catalyzed orthoester cyclization followed by Sonogashira cross-coupling. The experimentally determined HOMO values for these 4,8-disubstituted benzobisoxazoles ranged from -4.97 to -6.20 eV and showed reasonable correlation to the theoretically predicted values, with a percent deviation that ranged from 2.4–12.8%. However, the deviation between actual and predicted HOMO values was reduced to less than 3.5% when the theoretical values were extrapolated to the long-chain limit and compared to copolymers containing the 4,8-disubstituted benzobisoxazoles. Collectively, these results indicate that these 4,8-disubstituted *trans*-benzobisoxazoles can be used for the synthesis of new conjugated materials with electronic properties that are variable and predictable.



INTRODUCTION

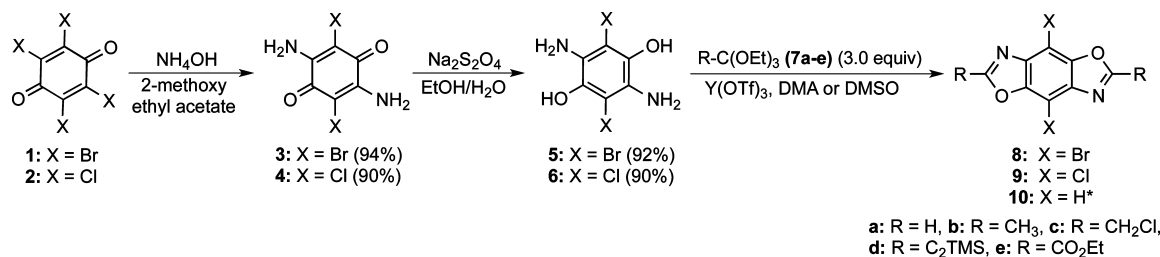
Conjugated polymers (CPs) are currently being investigated as replacements for traditional inorganic materials in applications such as field effect transistors (FET)s,^{1–5} organic light emitting diodes (OLED)s,^{6–8} and photovoltaic cells (PVC)s.^{9–12} The development of these organic semiconductors is motivated by the potential to reduce the cost of device fabrication through the use of solution-based techniques, and the ability to tune the energy levels for specific applications through chemical synthesis.¹³ Currently, a common approach for tuning the properties of CPs is through the synthesis of materials composed of alternating electron-donating and electron-accepting moieties.^{14–17} By varying the strength of the donor and acceptor components in the polymer backbone, the highest occupied molecular orbital (HOMO), lowest unoccupied molecular orbital (LUMO), and band gap of the resulting polymer can be readily manipulated.^{15,18} Since there are many known π -systems, a wide range of energy levels can be obtained by combining different components. However, in practice, certain combinations of properties such as electron-donating and hole-transporting materials (*p*-type) with low-lying LUMO levels and narrow band gaps or electron-accepting and electron-transporting materials (*n*-type) with good solubility are more difficult to attain. Thus, the design of new electron-rich or electron-poor building blocks remains a flourishing area of research.¹³

In this respect, benzobisoxazoles (BBOs) are promising electron-deficient heterocycles for the development of new

polymers because of their near-planar structure which can facilitate efficient packing and charge transport.^{19–22} Recently, BBOs have been used for the synthesis of donor–acceptor conjugated polymers; however, because of the relatively weak electron-accepting nature of the BBO moiety, the resulting materials have had fairly wide bands gaps (1.9–2.3 eV).^{23–25} Since BBO has two positions on the central benzene ring (4- and 8-) available for structural modification, it may be possible to design new derivatives that are better electron acceptors. In this paper, we evaluate alkyne substitution as an approach to increase electron affinity. We investigated the use of alkynes since, according to the Pauling scale, their electronegativity is similar to that of the cyano group (3.3), which has been widely used in the synthesis of electron-deficient building blocks.²⁶ Alkynes have also been utilized to alter the electronic properties of conjugated materials.^{27–34} In addition, alkynes offer the advantage of facile installation via Sonogashira cross-coupling. In the case of the BBO moiety, the additional structural variation through substitution facilitates the efficient synthesis of materials with tunable electronic properties by using shared synthetic intermediates. Herein, we examine the influence of alkyne substitution at the central benzene ring on the optical and electronic properties of 4,8-disubstituted benzo[1,2-*d*;4,5-*d'*]bisoxazoles (BBO)s, using a combination of synthetic and computational techniques.

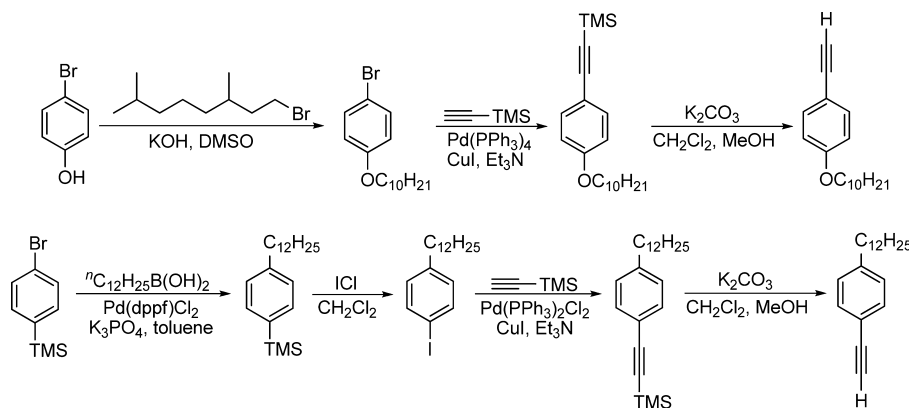
Received: June 9, 2011

Published: October 4, 2011

Scheme 1. Synthesis of 2,6-Disubstituted-4,8-dihalogenated BBOs^a

^a10b was synthesized according to the literature procedure.³⁵

Scheme 2. Synthesis of Substituted Phenylacetylenes



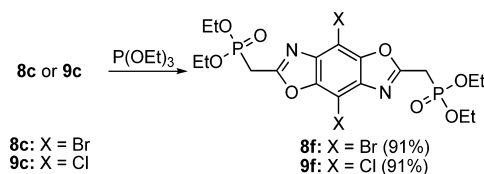
RESULTS AND DISCUSSION

Model Compound Synthesis. The synthesis of 4,8-dihalogenated-2,6-disubstituted BBOs is shown in Scheme 1. Recently, we reported a simple method for the synthesis of 2,6-disubstituted BBOs that occurs readily at low temperatures and is tolerant of a number of functional groups.³⁵ Utilizing this method and the halogenated diaminohydroquinones **5** and **6** we were able to synthesize several 4,8-dichloro- and 4,8-dibromo-2,6-disubstituted BBOs in good yields. The lowest yields were observed when ethyl triethoxyacetate (**7e**) was used for the synthesis of **8e** and **9e**. The reduction in yield is likely due to the poor nucleophilic site adjacent to the ester group. Although this reaction proceeded slowly, the moderate yields obtained (26–41%) are higher than previously reported values.²¹ We also modified the synthesis of **8d** and **9d** by using THF as the solvent due to the limited solubility of triethyl orthopropionate (**7d**) in DMA or DMSO. In all cases, the products were easily isolated by precipitation of the reaction mixture in water, filtration, followed by recrystallization from an appropriate solvent. Because of the scalable nature of the reactions, several compounds were prepared in multigram quantities without a decrease in yield.

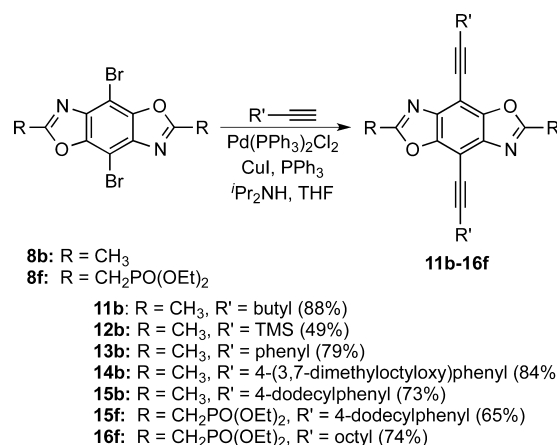
The synthesis of the 4-alkyl and 4-alkoxyphenylacetylenes is shown in Scheme 2. The flexible side chains were appended to improve the solubility of the resulting BBOs. The corresponding 4,8-bisalkynyl BBOs **11b**, **13b**, **14b**, **15b**, **15f**, and **16f** were obtained in good yields (73% to 88%) with **12b** in a lower yield (49%) by the Sonogashira cross-coupling reaction of 4,8-dibromo-2,6-dimethyl BBO **8b** and various alkynes as shown in Scheme 4.

The resultant substituted BBOs were fully characterized by ¹H NMR, ¹³C NMR, and high-resolution mass spectroscopy. For the most part, all attempts to grow crystals of the

Scheme 3. Synthesis of Bis(phosphonate) Esters by Arbuzov Reaction

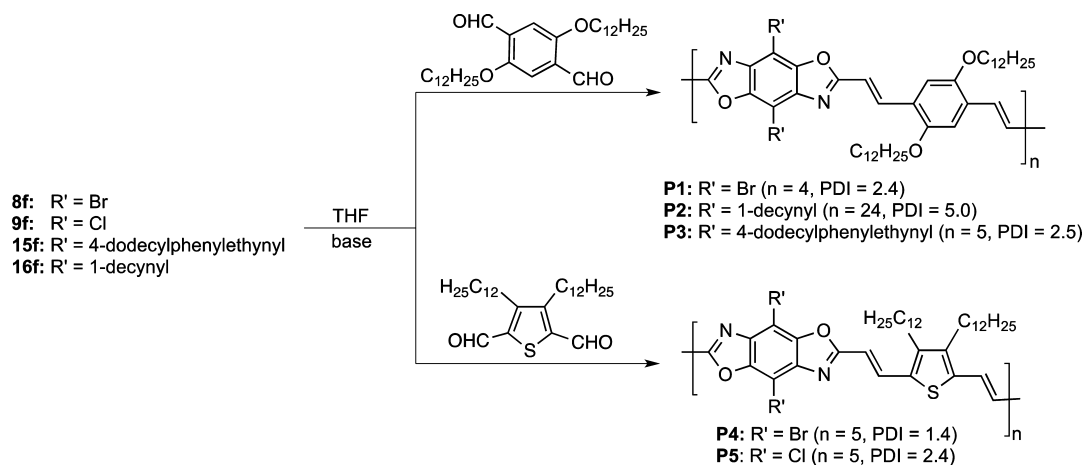


Scheme 4. Modification of 4,8-Dibromobenzobisoxazoles by Sonogashira Cross-Coupling



benzobisoxazoles via recrystallization or slow solvent evaporation produced either powders or small crystals that were unsuitable for X-ray crystallography. However, we were able to obtain suitable crystals of **8c**, **9a**, **9c**, and **10a** (see the crystallographic data in the Supporting Information).

Scheme 5. Synthesis of Benzobisoxazole Polymers



Polymer Synthesis. The synthesis of the 4,8-disubstituted poly(arylene vinylene benzobisoxazole)s is shown in Scheme 5. The bis(phosphonate) esters **8f** and **9f** were synthesized by the Arbuzov reaction of the corresponding 2,6-bis(chloromethyl) BBOs **8c** and **9c** and triethyl phosphite as shown in Scheme 3.²³ The bis(phosphonate) esters **15f** and **16f** were synthesized as shown in Scheme 4 by Sonogashira cross-coupling of **8f** with 1-decyne and 4-dodecylphenylacetylene, respectively. The Horner–Wadsworth–Emmons (HWE) polymerization of BBO monomers **8f**, **15f**, or **16f** and 2,5-didodecyloxyterephthalaldehyde³⁶ produced polymers **P1**, **P2**, and **P3** in yields of 56%, 87%, and 55%, respectively. Similarly, the HWE polymerization of BBO monomers **8f** or **9f** and 3,4-didodecylthiophene dicarboxaldehyde³⁷ yielded the corresponding polymers **P4** and **P5** in yields of 61% and 55%, respectively. **P1**, **P3**, **P5**, and **P6** were polymerized using potassium *tert*-butoxide as the base. The base-sensitive propargyl position on **16f** required the use of a LiBr/Et₃N for selective deprotonation of the phosphonate ester to obtain **P2** in 87% yield.³⁸ All of the polymers were soluble in several organic solvents, and the structures of the polymers were verified by ¹H NMR spectroscopy (see the Supporting Information) and gel permeation chromatography, which revealed monomodal molecular weight distributions.

Spectroscopic Characterization of Model Compounds. The UV–vis absorption (Figure 1) and photoluminescence (PL) (S50 Supporting Information) properties of the BBOs in solution have been investigated, and the spectral data are summarized in Table 1. The absorption and PL spectra vary depending on the type of substituents present on the 4,8-position of the BBO core. When excited at their respective λ_{\max} BBOs **8b**, **9b**, and **10b** exhibited very weak fluorescence in solution, whereas all of the other BBOs exhibited strong fluorescence in solution. The lack of fluorescence for **8b** and **9b** is likely due to the heavy-atom effect. The absorbance spectra of the halogen-substituted BBOs **8b** and **9b** displayed intense vibronic coupling with three dominant absorption bands, whereas the unsubstituted BBO **10b** had two major peaks, each showing strong vibronic coupling. The absorbance spectra of the ethynyl-substituted BBOs **11b**–**15b** displayed weak vibronic coupling. All of the substituted BBOs had red-shifted absorbance spectra due to the extended conjugation of the system relative to the unsubstituted BBO **10b** (abs λ_{\max} 209, 285 nm). The phenylethynyl benzobisoxazoles **13b**–**15b** featured longer conjugation lengths and thus absorbed at the

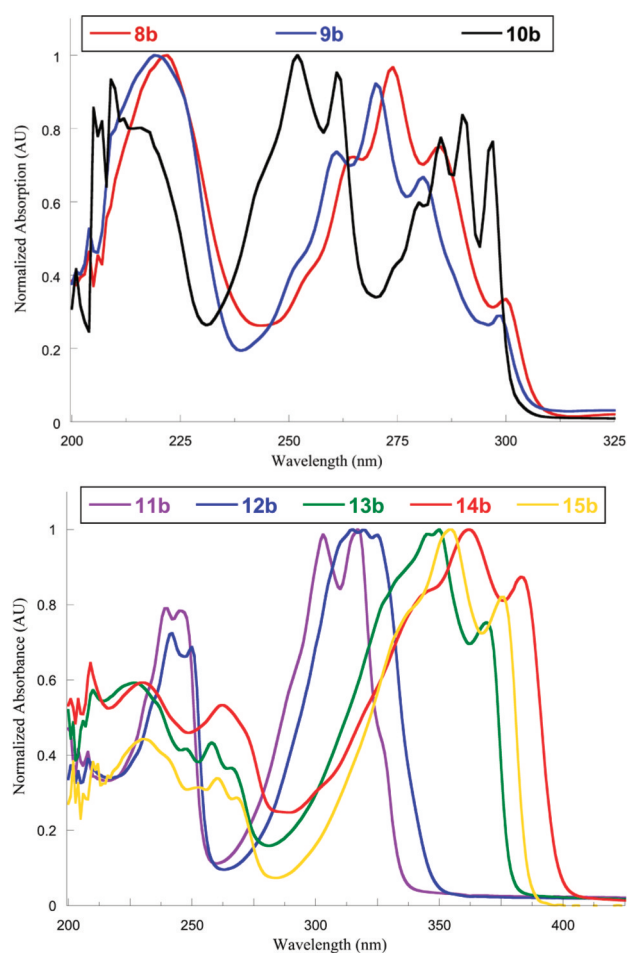


Figure 1. UV–vis spectra of parent and halogenated BBOs (top) and alkyne substituted BBOs (bottom).

longest wavelengths. The introduction of the alkoxy-group onto the *para* position of the phenyl substituent resulted in a red shift in the absorbance spectrum; consequently, **14b** absorbed at a longer wavelength than **15b**.

The PL and absorption spectra of the polymers in solution (Figure 2) and in thin film (S52 Supporting Information) were also measured. In solution, **P1** had a PL maximum at 524 nm, with absorption maximum at 476 nm. **P4** had a PL maximum at 563 nm, with an absorption maximum at 506 nm, and **P6** had a

Table 1. Optical Data of BBO Model Compounds

	λ_{abs} (nm) ^a	ϵ^b (M ⁻¹ cm ⁻¹)	λ_{ems} (nm)
8b	222*, 274	38900	307, 385
9b	219*, 274	23600	313, 385
10b	209, 252*, 285	16200	308, 401
11b	243, 304, 317*	38700	348
12b	242, 315*	33600	362
13b	248, 350*, 369	43600	376
14b	226, 259, 362*, 383	45600	397
15b	229, 355*, 376	58600	383

^aAll measurements performed in THF. ^bExtinction coefficients based on absorbance at λ_{max} . ^cPerformed at λ_{max} . Asterisk (*) denotes λ_{max} .

PL maximum at 560 nm, with an absorption maximum at 510 nm. When the dialkoxyphenyl comonomer was replaced with the less aromatic and more electron-rich dialkylthiophene, a red shift in the absorbance spectra occurred. In all cases, the PL and absorption spectra were very similar to the analogous nonhalogenated polymers: poly(2,5-bisdodecyloxyphenylene vinylene)-*alt*-benzo[1,2-*d*;4,5-*d'*]bisoxazole]-2,6-diyl²³ and poly(3,4-didodecylthiophene vinylene)-*alt*-benzo[1,2-*d*;4,5-*d'*]bisoxazole]-2,6-diyl.²⁴ The alkyl-alkyne substituted polymer P2 had a PL maximum at 576 nm, with absorption maximum at 491 nm, whereas the phenylethynyl substituted P3 had a PL maximum at 601 nm with an absorption maximum at 520 nm. The bathochromic shift in the absorbance spectra of these polymers relative to their halogenated counterparts was a result of the increased acceptor strength of the substituted BBOs.

The energy levels of the BBO model compounds were investigated and compared to the theoretical data (see Table 2). The HOMO values obtained for 8b–10b using cyclic voltammetry had excellent correlation to those predicted by theory, with a percent error of less than 5%. However, we saw a large deviation between the electrochemically determined HOMO values and the predicted values for the other BBOs. As a whole, the electrochemistry of the BBOs was not well behaved and all molecules exhibited nonreversible oxidation cycles. Furthermore, a reduction cycle was not seen for any of the compounds within the solvent window for the acetonitrile/Bu₄N⁺BF₄⁻ (-2.7 to -3.0 eV versus Ag/AgCl). For this reason, we evaluated the BBOs using ultraviolet photoelectron spectroscopy (UPS), which provides an absolute determination

of the HOMO level.^{39–41} The UPS HOMO values of the BBOs ranged from -5.70 to -6.50 eV, and the experimentally determined band gaps ranged from 3.19 to 4.62 eV. The LUMO levels ranged from -1.28 to -2.59 eV, and were calculated by adding the optical band gap to the HOMO values. The introduction of electron-withdrawing groups into π -conjugated systems stabilized the LUMO energy and increased the electron-transporting ability.³ In general, the alkynyl substituted BBOs had deeper HOMOs and smaller band gaps than the halogenated BBOs. When a phenyl ring was added onto the alkynyl substituent, the HOMO level was slightly decreased, and the LUMO level was slightly increased in comparison to the unsubstituted alkynyl group. The HOMO was further raised when electron-donating alkyl or alkoxy substituents were added to the ring.

Computational Studies. To elucidate the influence of structural modification on the optical and electronic properties of the 4,8-disubstituted BBOs, ground-state geometry optimizations were performed utilizing density functional theory (DFT) employing a B3LYP⁴² functional, a 6-31G* basis and the Gaussian 03W software package. DFT/B3LYP/6-31G* is a reliable method that has been widely used for calculating the structural and optical properties of many systems.^{43–46} UV-vis spectra were simulated utilizing the first 10 excited states and the time-dependent density functional theory (TDDFT) routine with the aforementioned functional and basis set (see Figure 4 and the Supporting Information). In addition, the HOMO, LUMO, and optical band gaps (the first excited state) were produced from the TDDFT output. To minimize computational cost, methyl groups were used at the 2 and 6 positions. Also, all alkoxy side chains were truncated to methoxy side chains and alkyl side chains omitted. Hence, the results for structure 15b are not reported here since it would be a replication of the prediction for structure 13b. To evaluate the predictive power of the computational method, a comparison of computed HOMO, LUMO, and optical band gap values to experimental data was made. These results are summarized in Table 2.

There was a good correlation for BBOs without conjugated substituents (8b–10b), such that the difference between the theoretical and the experimental values for the HOMOs was less than 0.3 eV. However, the difference between predicted and measured values was as large as 0.8 eV for the optical band

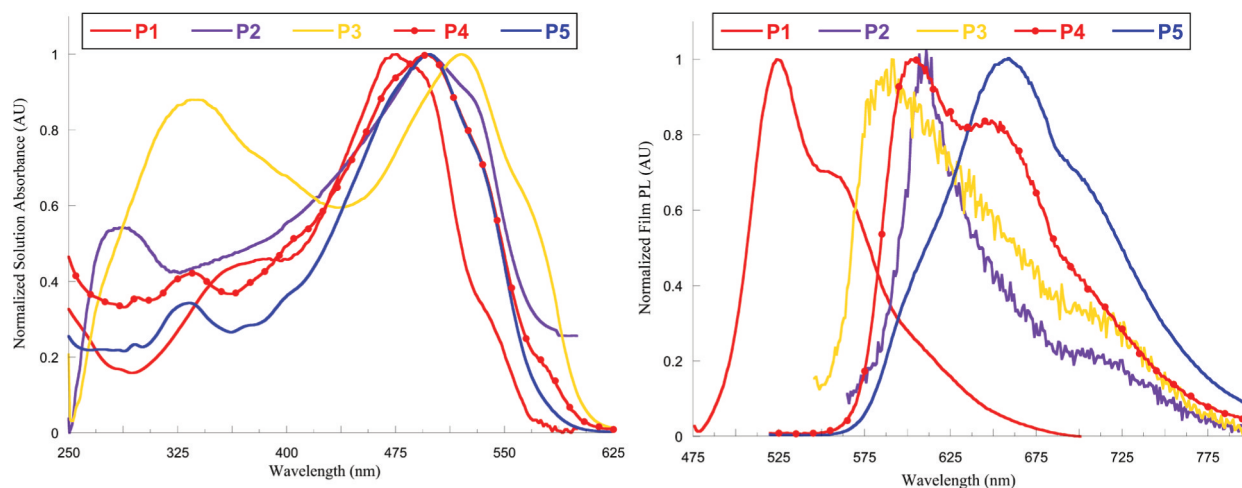


Figure 2. UV-vis spectra of polymers: in solution and as films spun from THF or chloroform/*o*-dichlorobenzene solutions (right).

Table 2. Experimental and Theoretical Comparison of the Electronic Properties of BBO Model Compounds

	HOMO (eV)			LUMO (eV)			E_g^{opt} (eV)		
	expt ^a	theory	% dev	expt ^b	theory	% dev	expt	theory	% dev
8b	-6.50	-6.20	4.6	-2.28	-1.45	36.4	4.22 (294) ^c	4.42	4.7
9b	-6.50	-6.30	3.1	-2.16	-1.47	31.9	4.34 (286) ^d	4.52	4.1
10b	-5.90	-6.04	2.4	-1.28	-1.01	21.1	4.62 (296) ^d	4.70	1.7
11b	-5.93	-5.40	8.9	-2.24	-1.43	36.2	3.69 (336) ^d	3.84	4.1
12b	-6.09	-5.70	6.5	-2.47	-1.81	26.7	3.62 (343) ^d	3.74	3.3
13b	-5.92	-5.30	10.5	-2.65	-1.97	25.7	3.27 (379) ^d	3.16	3.4
13b^e		-5.67	4.3		-1.67	37.0		3.76	18.0
14b	-5.70	-4.97	12.8	-2.58	-1.74	32.6	3.12 (398) ^d	3.03	2.9
14b^e		-5.54	2.9		-1.54	40.3		3.41	9.3
15b	-5.78	n/a	n/a	-2.59	n/a	n/a	3.19 (386) ^d	n/a	n/a

^aDetermined using ultraviolet photoelectron spectroscopy. ^bCalculated from HOMO - E_g^{opt} . ^cMeasured from the λ_{max} absorbance. ^dCalculated from lowest energy absorption onset from the intersection of the leading edge tangent with the x -axis. ^eBased on an optimized geometry of 90°.

gaps. This was not surprising as DFT methods are known to underestimate band gaps.^{47–50} The difference between the theoretical and the experimental values for the LUMOs was as large as 0.4 eV. These values possessed the highest amount of deviation (12–58%) due to the propagated deviations in the optical band gap and the HOMO values. A larger deviation in theoretical and experimental HOMO values was observed for BBOs bearing alkynyl substituents. The deviation was moderate for structures **11b** and **12b** (0.53 and 0.39 eV), whereas the variance in structures **13b** and **14b** was much higher (0.62 and 0.73 eV). We hypothesized that the optimized geometry could be the source of error for the phenylethynyl substituted structures. The minimized geometry predicted a planar configuration whereas it is likely the actual compounds possessed rings that were twisted out of plane. The idea of nonplanarity in phenylethynyl side chains is supported by a number of studies.^{51,52} To validate this hypothesis, optimized geometries and subsequent excited-state calculations were performed on structures in which the phenyl substituent was forced perpendicular to the BBO core (see Figure 3). Adapting

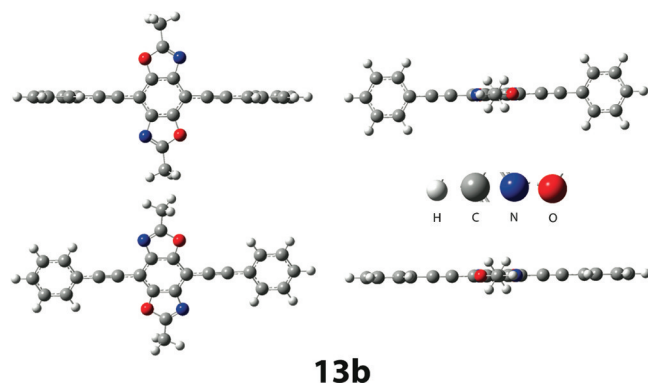


Figure 3. Representation for the optimized (bottom) and perpendicular (top) geometries of **13b**.

a twisted geometry reduced the large deviation between the experimental and theoretical HOMO values for **13b** and **14b** from 0.62 to 0.25 eV and from 0.73 to 0.16 eV, respectively.

Strong correlation between the experimental and simulated UV-vis spectra was also observed. A direct comparison for **12b** is shown in Figure 4, and the remaining structures are shown in the Supporting Information (Figures S53–S58). The gray and black lines represented the experimental data and theoretical fit,

respectively. The black bars and solid squares were indicative of the oscillator strength and the corresponding excited state. There was a very good agreement between the two data sets especially when one considers that all theoretical computations were performed in vacuum and did not account for solvent stabilization that was present in the experimental sample. This was further demonstrated in an analysis of the contributions of the excited states (see Supporting Information).⁵³ In all cases, the lowest lying state was primarily due to electronic excitations directly between the HOMO and the LUMO. For **8b**, **9b**, and **12b**, this lowest state was split into two excited states in the computed spectra, whereas the experimental spectra displayed one broad peak. To further evaluate the competency of this method, we generated a correlation plot of the observed and computed wavelengths (see Figure 4). For this comparison, an

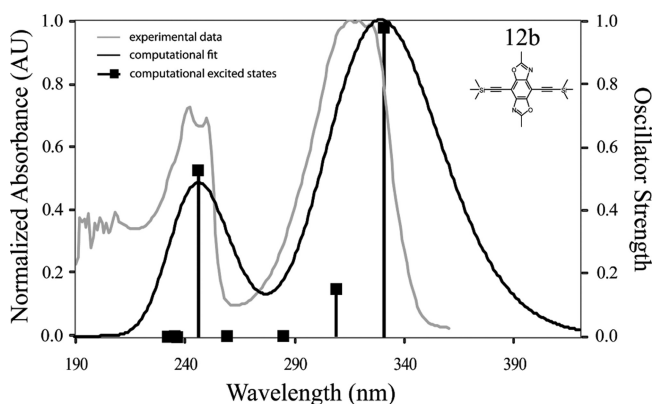


Figure 4. Comparison of the experimental UV-vis spectrum of **12b** with the predicted excited states.

R^2 value of 0.87 was found, indicating good correlation between the experimental and theoretical values.

To examine the influence of substitution on the electron density of the BBO core, the frontier orbitals and electrostatic potential (ESP) maps for each of the model compounds were generated and are shown in Figure 6. The electron-withdrawing nature of the halogens is demonstrated by the frontier orbital HOMOs for **8b** and **9b**, which show a significant amount of electron density that has been drawn away from the BBO backbone. This effect was further exhibited by the ESP maps in which the backbone is slightly greener (less electron rich) than that of the unsubstituted core **10b**. Similarly, the electron-withdrawing alkynyl substituents also exhibited a reduction in

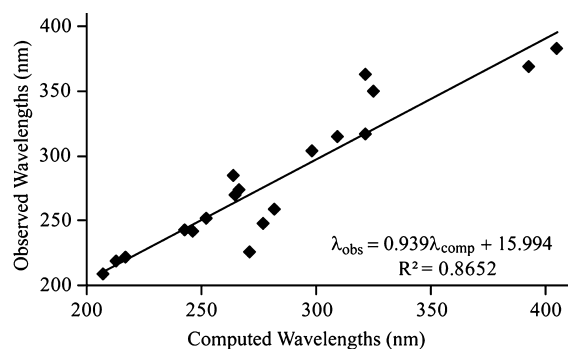


Figure 5. Correlation plot of the observed and computed wavelengths.

the density of the BBO core (see **11b**, **12b**, **13b**, and **14b**). However, the addition of substituents bearing phenyl rings led to a large reorganization of electron density from the BBO core (see **13b** and **14b**). This redistribution was so significant that it appears that the BBO core was no longer the primary conjugation axis, which is noteworthy because it suggests that alkynyl substitution can be used in the synthesis of two-dimensional π -delocalized polymers. Such cruciforms can exhibit interesting optical and electronic properties due to their multiple conjugated pathways.^{20,22,54–57}

The ability to accurately predict the electronic properties of polymeric materials is essential for the design of new organic

semiconductors. To evaluate the ability of our computational methods to predict the properties of 4,8-disubstituted BBO polymers, the geometries of model oligomers ($n = 1, 2, 3,$ and 4) for **P1**, **P2**, **P3**, **P4**, and **P6** were optimized at the density functional theory B3LYP/6-31G* level. In all cases, the bisdodecyl substituents were truncated to methyl groups to reduce computational costs. Unfortunately, **P3** was found to be too large to extrapolate to the long-chain limit. The HOMO, LUMO and band gaps for these polymers were obtained by fitting the aforementioned set of oligomers with the Kuhn expression^{58,59}

$$E = E_0 \sqrt{1 + 2 \frac{k'}{k_0} \cos \frac{\pi}{N+1}} \quad (1)$$

where E_0 is the transition energy of a formal double bond, N is the number of double bonds in the oligomer, and k'/k_0 is an adjustable parameter. The results are summarized in Table 3. Overall, there was excellent correlation between all predicted and experimental values. The largest deviation for both the HOMO and LUMO levels were 1.5% and 4.0%, respectively. This trend was quite an improvement over the small molecule cases where the deviation was quite a bit larger (12.8% for HOMO and 40.3% for LUMO). The polymeric band gaps were found to experience the largest amount of deviation at 10.7%, which was attributed to DFT overestimation.^{43,46} As a whole, these results indicated that this level of theory can be used to

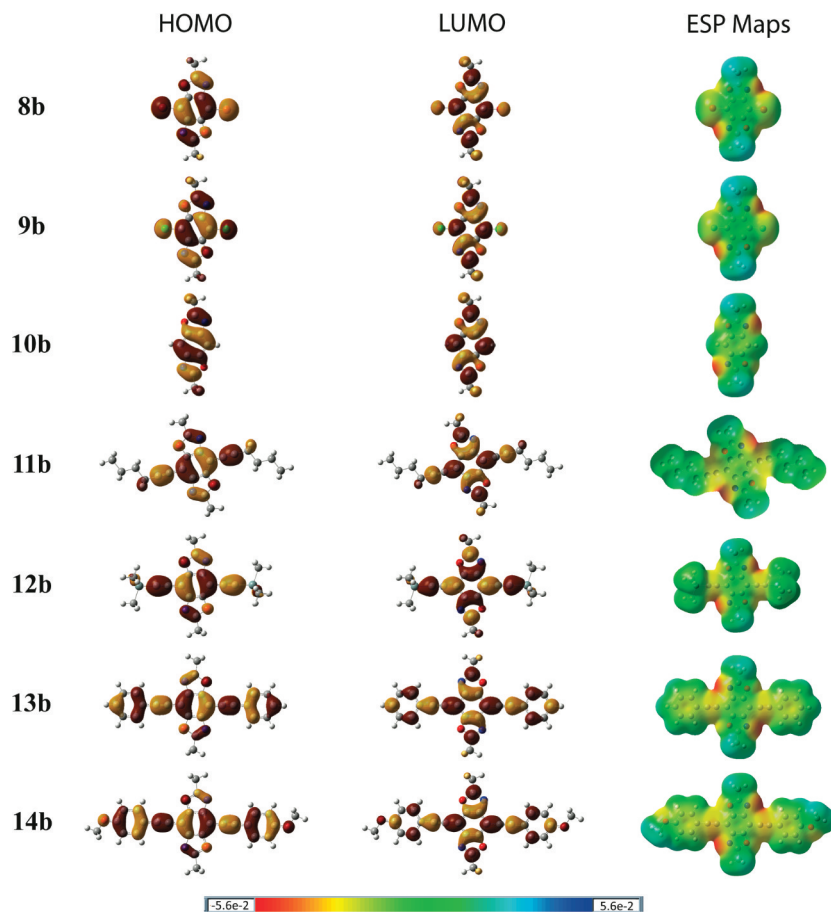


Figure 6. Pictorial representations of the frontier orbitals for compounds **8b**–**14b** (left) and electrostatic potential maps (right). For the frontier orbitals, the red lobes are positive and the yellow lobes are negative. The charge density within the electrostatic potential maps range from red (electron rich) to blue (electron poor).

Table 3. Experimental and Theoretical Comparison of the Electronic Properties of BBO Polymers

	HOMO (eV)			LUMO (eV)			E_g^{opt} (eV)		
	expt	theory	% dev	expt	theory	% dev	expt	theory	% dev
P1	-5.06 ^a	-5.23	3.4	-2.91 ^b	-2.93	0.7	2.15 ^c	2.03	5.6
P2	-5.05 ^a	-4.98	1.4	-3.00 ^b	-2.78	4.0	2.05 ^c	1.98	3.4
P3	-5.00 ^a	n/a	n/a	-2.96 ^b	n/a	n/a	2.04 ^c	n/a	n/a
P4	-5.38 ^a	-5.43	0.93	-3.30 ^b	-3.23	2.1	2.05 ^c	1.92	6.3
P5	-5.38 ^a	-5.46	1.5	-3.31 ^b	-3.26	1.5	2.07 ^c	1.91	7.7

^aCalculated from LUMO - E_g^{opt} . ^bMeasured in degassed CH₃CN using 0.1 M Bu₄NPF₆, referenced to Fc/Fc⁺ (HOMO level -4.8 eV below vacuum). Measured from the absorbance at λ_{max} . ^cCalculated by the energy absorption onset from the intersection of the leading edge tangent with the x -axis.

accurately predict the HOMO, LUMO, and band gaps for conjugated polymers possessing BBO moieties.

CONCLUSIONS

In summary, we have demonstrated that alkyne substitution at the central benzene ring of benzo[1,2-*d*;4,5-*d'*]bisoxazoles can be used to modify the optical and electronic properties of these compounds. We were able to synthesize the target compounds in good yields by first synthesizing halogenated benzobisoxazoles and then forming two-dimensional π -systems using Sonogashira cross-coupling. The predicted HOMO values for the small molecules matched well with the experimental results, although as expected, a higher degree of error was seen for the LUMO and band gap values. In contrast, the predicted energy levels for polymeric materials exhibited excellent correlation for all parameters, further exemplifying the usefulness of the theoretical methods for designing new materials. Although theoretical calculations predicted that attachment of alkynes could be used to vary the energy levels of BBOs by almost 1 eV, smaller changes were observed for the BBO polymers. While it was our intention to minimize computational requirements by using small molecules to evaluate the impact of these structural modifications, this was unfortunately not reasonable as it appears that most of the electronic tuning in BBO small molecules was due to a change in the conjugation axis. Currently, we are designing new BBOs bearing other electron withdrawing groups to further improve the acceptor strength of this group and synthesizing new conjugated polymers based on these alkyne substituted BBOs.

EXPERIMENTAL SECTION

General Methods. Unless otherwise noted, reactions were conducted under ambient atmosphere at 18–26 °C. Nuclear magnetic resonance (NMR) experiments were carried out in either CDCl₃ or DMSO-*d*₆ at 400 MHz (¹H) or 100 MHz (¹³C). ¹H NMR spectra are internally referenced to the residual protonated solvent peak, and the ¹³C NMR are referenced to the central carbon peak of the solvent. In all spectra, chemical shifts are given in δ relative to the solvent. Coupling constants are reported in hertz (Hz). Cyclic voltammetry was performed using a potentiostat, scanning at a rate of 50–100 mV/s. The polymer solutions (2–10 mg/mL) were drop-cast on a platinum electrode, and Ag/Ag⁺ was used as the reference electrode. The reported values are referenced to Fc/Fc⁺ (-4.8 eV versus vacuum). All electrochemistry experiments were performed in dry-degassed CH₃CN under argon atmosphere using 0.1 M tetrabutylammonium hexafluorophosphate as the electrolyte. High-resolution mass spectra were recorded on a double-focusing magnetic sector mass spectrometer using EI or ESI at 70 eV. Melting points were obtained using a melting point apparatus, upper temperature limit 260 °C. Gel permeation chromatography (GPC) measurements were performed on a separation module equipped with three 5 μ m I-gel columns connected in a series (guard, HMW, MMW, and LMW) with a UV-

vis detector. Analyses were performed at 35 °C using THF as the eluent with the flow rate at 1.0 mL/min. Calibration was based on polystyrene standards. Fluorescence spectroscopy and UV-visible spectroscopy were obtained using polymer solutions in THF, and thin films were spun from THF or CHCl₃/*o*-dichlorobenzene solutions. The films were made by spin-coating 25 × 25 × 1 mm glass slides, using 10 mg/mL polymer solutions at a spin rate of 5000 rpm on a spin-coater. Ultraviolet Photoelectron Spectroscopy measurements were performed on sample films. X-ray radiation and the detector to crystal distance of 5.03 cm. X-ray crystal structure data for compounds 10a (CDC 734101), 10b (CCDC 687294), 10c (CCDC 734103), 10d (CCDC 734102), and 9c (CCDC 838477) were deposited with the Cambridge Crystallographic Data Centre, 12 Union Road, Cambridge CB2 1EZ, UK. Triethyl orthochochloroacetate (7c),⁶⁰ trimethylsilyl ethyl orthopropiolate (7d),³⁵ ethyl triethoxyacetate (7e),⁶¹ *p*-bromanil,⁶² 4-bromo-trimethylsilylbenzene,⁵ 2,6-dimethylbenzo[1,2-*d*;4,5-*d'*]bisoxazole (10b),³⁵ 2,5-didodecyloxyterephthalaldehyde,³⁶ and 3,4-didodecylthiophene dicarboxaldehyde³⁷ were prepared according to literature procedure.^{35,63} 3,6-Diamino-2,5-dichloro-1,4-benzoquinone was prepared from *p*-chloranil according to literature procedure.⁶²

3,6-Diamino-2,5-dibromo-1,4-benzoquinone (3). A 500 mL, three-neck round-bottom flask was equipped with an addition funnel and mechanical stirrer and charged with 42.9 g (100 mmol) of *p*-bromanil (1) and 170 mL of 2-methoxyethyl acetate. The slurry was vigorously stirred while heating to 60 °C. The mixture was removed from the heat source and the addition funnel charged with 43.3 mL (300 mmol) of 27% NH₄OH and added dropwise over 25 min (the reaction exothermed to over 100 °C during the addition). The reaction mixture was allowed to cool to approximately 80 °C, stirred at this temperature for 3 h, and allowed to cool to room temperature overnight. The dark red mixture was filtered and the collected precipitate washed with large portions of distilled water. The collected solid was placed in a flask containing acetone, stirred, and refiltered. The precipitate was then washed with acetone and dried in vacuo to yield a brick-red powder (27.9 g, 94% yield). Because of the limited solubility of this compound it was used without further purification or analysis.

3,6-Diamino-2,5-dibromo-1,4-hydroquinone (5). A 100 mL round-bottom flask equipped with a large stir bar was charged with 3.26 g (11.0 mmol) of 3,6-diamino-2,5-dibromo-1,4-benzoquinone (3), 33 mL of ethanol, and 7 mL of distilled water. The flask was fitted with an addition funnel and heated to 55 °C with stirring under argon atmosphere. The addition funnel was charged with 4.78 g (27.5 mmol) of Na₂S₂O₄ dissolved in 50 mL of distilled water, the solution added dropwise, and the mixture stirred for 1 h. The mixture was allowed to cool to room temperature and the precipitate filtered and washed with distilled water and cold ethanol. The resulting solid was dried in vacuo to yield a tan powder (3.07 g, 94% yield). Because of the insolubility and air sensitivity of this compound it was used immediately without further purification or analysis.

3,6-Diamino-2,5-dichloro-1,4-hydroquinone (6). Prepared analogously to 5 from 3,6-diamino-2,5-dichloro-1,4-benzoquinone (4) (11 mmol) to yield a light tan powder (2.30 g, 90% yield).

Because of the insolubility and air sensitivity of this compound it was used immediately without further purification or analysis.

Representative Procedure for the Preparation of 4,8-Dibromobenzobisoxazoles. A dry round-bottom flask was placed under an argon atmosphere and charged with 0.13 g (0.25 mmol) of $Y(OTf)_3$, 5 mL of DMA, and 3 equiv of orthoester 7a–e. The mixture was warmed to 55 °C, and 1.49 g (5.0 mmol) of 3,6-diamino-2,5-dibromo-1,4-hydroquinone (5) was added portionwise over 30 min and stirred at 55 °C for 2 h. The mixture was allowed to cool to room temperature and diluted with water. The resulting precipitate was collected by filtration and washed with distilled water and cold ethanol.

4,8-Dibromobenzo[1,2-*d*;4,5-*d'*]bisoxazole (8a; X = Br, R = H). Prepared from 5 (5 mmol) and triethyl orthoformate 7a. Purified by recrystallization from acetic acid to yield white needles, (0.77 g, 48% yield): mp > 260 °C; 1H NMR (400 MHz, DMSO- d_6) δ 9.05 (2H, s); ^{13}C NMR (100 MHz, DMSO- d_6) δ 92.4, 137.7, 145.7, 156.3; HRMS (ESI) calcd for $C_8H_3N_2O_2Br_2$ 316.8556 (M + H) $^+$, found 316.8558.

4,8-Dibromo-2,6-dimethylbenzo[1,2-*d*;4,5-*d'*]bisoxazole (8b; X = Br, R = CH₃). Prepared from 5 (20 mmol) and triethyl orthoacetate 7b. Purified by recrystallization from chloroform/ethanol to yield white needles (5.53 g, 85% yield): mp > 260 °C; 1H NMR (400 MHz, CDCl₃): δ 2.74 (6H, s); ^{13}C NMR (100 MHz, CDCl₃): δ 15.1, 92.1, 136.7, 146.8, 165.8; HRMS (EI) Calcd for $C_{10}H_6N_2O_2Br_2$, 343.87960 (M $^+$), found 343.88060.

4,8-dibromo-2,6-bis(chloromethyl)benzo[1,2-*d*;4,5-*d'*]bisoxazole 8c (X = Br, R = CH₂Cl). Prepared from 5 (30 mmol) and triethyl orthochloroacetate 7c. The crude product was heated in chloroform (500 mL) and filtered. The filtrate was concentrated to 200 mL diluted 1:1 with ethanol to obtain yellow needles (8.33 g, 70% yield): mp > 260 °C; 1H NMR (400 MHz, CDCl₃) δ 4.88 (4 H, s); ^{13}C NMR (100 MHz, CDCl₃) δ 36.0, 93.2, 138.3, 147.5, 163.2; HRMS (ESI) calcd for $C_{10}H_3N_2O_2Cl_2Br_2$ 412.8092 (M + H) $^+$, found 412.8089.

4,8-Dibromo-2,6-bis(trimethylsilylethynyl)benzo[1,2-*d*;4,5-*d'*]bisoxazole (8d; X = Br, R = C₂TMS). Prepared from 5 (3 mmol) and triethyl orthopropiolate 7d using THF in place of DMA and heated to 50 °C. The solvent was removed in vacuo and the crude product purified by recrystallization from heptanes to yield small yellow needles (0.96 g, 63% yield): mp 245 °C; 1H NMR (400 MHz, CDCl₃): δ 0.34 (18 H, s); ^{13}C NMR (100 MHz, CDCl₃): δ 0.7, 90.5, 92.4, 105.2, 139.5, 146.6, 148.3; HRMS (ESI) Calcd for $C_{18}H_{19}O_2N_2Si_2Br_2$, 508.9346 (M + H) $^+$, found 508.9348.

4,8-Dibromo-2,6-bis(ethyl acetyl)benzo[1,2-*d*;4,5-*d'*]bisoxazole (8e; X = Br, R = CO₂Et). Prepared from 5 (5 mmol) and ethyl triethoxyacetate 7e. Purified by recrystallization from chloroform/heptanes to yield pale yellow needles (0.59 g, 26% yield): mp > 260 °C; 1H NMR (400 MHz, CDCl₃) δ 1.54 (6H, t, J = 8 Hz), 4.62 (4H, q, J = 8 Hz); ^{13}C NMR (100 MHz, CDCl₃) δ 23.6, 57.0, 93.5, 123.89, 151.1, 154.3, 157.3; HRMS (ESI) calcd for $C_{14}H_{11}N_2O_6Br_2$, 460.8978 (M + H) $^+$, found 460.8975.

Representative Procedure for the Preparation of 4,8-Dichlorobenzobisoxazoles. A dry round-bottom flask was placed under an argon atmosphere and charged with 0.13 g (0.25 mmol) of $Y(OTf)_3$, 5 mL of DMSO, and 3 equiv of orthoester 7a–e. The mixture was warmed to 55 °C, 1.05 g (5.00 mmol) of 3,6-diamino-2,5-dichloro-1,4-hydroquinone (6) was added portionwise over 30 min, and the mixture was stirred at 55 °C for 2 h. The mixture was allowed to cool to room temperature and diluted with water. The resulting precipitate was collected by filtration and washed with water and cold ethanol.

4,8-Dichlorobenzo[1,2-*d*;4,5-*d'*]bisoxazole (9a; X = Cl, R = H). Prepared from 6 (5 mmol) and 7a. Purified by recrystallization from chloroform to yield small white needles (1.56 g, 84% yield): mp > 260 °C; 1H NMR (400 MHz, DMSO- d_6) δ 9.07 (2H, s); ^{13}C NMR (100 MHz, DMSO- d_6) δ 104.4, 136.5, 144.3, 156.6; HRMS (ESI) calcd for $C_8H_3N_2O_2Cl_2$, 228.9566 (M + H) $^+$, found 228.9572.

4,8-Dichlorobenzo-2,6-dimethylbenzo[1,2-*d*;4,5-*d'*]bisoxazole (9b; X = Cl, R = CH₃). Prepared from 6 (20 mmol) and 7b. Purified by recrystallization from chloroform/ethanol to yield white needles (0.78 g, 79% yield): mp > 260 °C; 1H NMR (400 MHz,

CHCl₃) δ 2.75 (6 H, s); ^{13}C NMR (100 MHz, CHCl₃) δ 15.1, 104.0, 137.5, 145.5, 166.1; HRMS (ESI) calcd for $C_{10}H_7N_2O_2Cl_2$, 256.9879 (M + H) $^+$, found 256.9881.

4,8-Dichloro-2,6-bis(chloromethyl)benzo[1,2-*d*;4,5-*d'*]bisoxazole (9c; X = Cl, R = CH₂Cl). Prepared from 6 (20 mmol) and 7c. Purified by recrystallization from chloroform/ethanol to yield yellow needles (4.69 g, 74% yield): mp 233–234 °C; 1H NMR (400 MHz, CHCl₃) δ 4.84 (4H, s); ^{13}C NMR (100 MHz, CHCl₃): δ 23.6, 106.0, 117.6, 138.1, 146.1, 163.4; HRMS (ESI) calcd for $C_{10}H_3N_2O_2Cl_4$ 324.9103 (M + H) $^+$, found 324.9100.

4,8-Chloro-2,6-bis(trimethylsilylethynyl)benzo[1,2-*d*;4,5-*d'*]bisoxazole (9d; X = Cl, R = C₂TMS). Prepared from 6 (3 mmol) and 7d using THF in place of DMSO and heating to 50 °C. The solvent was removed in vacuo and the crude product purified by recrystallization from heptanes to yield pale yellow needles (0.73 g, 58% yield): mp 232–234 °C; 1H NMR (400 MHz, CDCl₃) δ 0.34 (18 H, s); ^{13}C NMR (100 MHz, CDCl₃) δ 0.2, 90.4, 105.2, 105.3, 138.3, 145.3, 148.6; HRMS (ESI) calcd for $C_{18}H_{19}N_2O_2Si_2$ 421.0357 (M + H) $^+$, found 421.0350.

4,8-Dichloro-2,6-bis(ethylacetyl)benzo[1,2-*d*;4,5-*d'*]bisoxazole (9e; X = Cl, R = CO₂Et). Prepared from 6 and 7e. Purified by recrystallization from chloroform/ethanol to yield light yellow needles (0.46 g, 41% yield): mp > 260 °C; 1H NMR (400 MHz, CDCl₃) δ 1.52 (6 H, t, J = 8 Hz), 4.62 (4 H, q, J = 8 Hz); ^{13}C NMR (100 MHz, CDCl₃) δ 14.4, 64.3, 108.2, 139.2, 146.3, 155.0, 155.4; HRMS (ESI) calcd for $C_{14}H_{11}N_2O_6Cl_2$ 372.9989 (M + H) $^+$, found 372.9992.

1-(3,7-Dimethyloctyloxy)-4-ethynylbenzene. 1-Bromo-4-(3,7-dimethyloctyloxy)benzene. A 250 mL round-bottom flask was charged with 100 mL of DMSO and 7.0 g (125 mmol) of KOH and stirred for 1 h at room temperature. Then 17.3 g (100 mmol) of 4-bromophenol and 27.6 g (125 mmol) of 1-bromo-3,7-dimethyloctane were added successively, and the reaction mixture stirred at room temperature overnight. The mixture was poured into 200 mL of water and extracted with dichloromethane (3 \times). The combined organic layers were washed with 2 N HCl (3 \times) and brine (1 \times) and dried over MgSO₄. The solution was filtered and the solvent removed in vacuo. Distillation of the crude product under reduced pressure (185 °C, 260 mTorr) yielded a clear oil (31.0 g, 95% yield): 1H NMR (400 MHz, CDCl₃) δ 0.87 (6H, d, J = 8 Hz), 0.96 (3H, d, J = 8 Hz), 1.15–1.87 (10H, overlapping multiplets), 3.96 (2H, sextet, J = 8 Hz), 6.79 (2H, d, J = 8 Hz), 7.37 (2H, d, J = 12 Hz); ^{13}C NMR (400 MHz, CDCl₃) 20.0, 22.8, 28.2, 30.0, 36.3, 37.5, 39.4, 66.7, 112.7, 116.5, 132.3, 158.4; HRMS (EI) calcd for $C_{16}H_{25}OBr$ 312.1089 (M $^+$), found 312.1084.

1-(3,7-Dimethyloctyloxy)-4-(trimethylsilylethynyl)benzene. A dry pressure flask was sealed with a septum, equipped with a stir bar, and purged with argon. The flask was charged with 50 mL of dry/degassed Et₃N and 3.29 g (10.0 mmol) of 1-(3,7-dimethyloctyloxy)-4-bromobenzene, 0.35 g (0.30 mmol) of Pd(PPh₃)₄ and 0.038 g (0.20 mmol) of CuI followed by 1.28 g (13.0 mmol) of trimethylsilylacetylene. The flask was sealed with a Teflon cap and heated to 80 °C for 24 h. The solution was cooled to room temperature, diluted with water, and extracted with hexanes (4 \times). The combined organic extracts were washed with water (2 \times) and brine (2 \times) and dried over MgSO₄. The solution was filtered and the solvent removed in vacuo. The product was purified by column chromatography eluting with hexanes/ethyl acetate (98:2) to yield a clear oil (1.62 g, 47% yield): 1H NMR (400 MHz, CDCl₃) δ 0.24 (9H, s), 0.88 (6H, d, J = 8 Hz), 0.94 (3H, d, J = 8 Hz), 1.15–1.89 (10H, overlapping multiplets), 3.98 (2H, m), 6.82 (2H, d, J = 12 Hz), 7.39 (2H, d, J = 12 Hz); ^{13}C NMR (100 MHz, CDCl₃) δ 19.9, 22.9, 24.9, 28.2, 30.0, 36.3, 37.49, 39.45, 66.6, 92.4, 105.5, 114.5, 115.16, 133.6, 159.5.

1-(3,7-Dimethyloctyloxy)-4-ethynylbenzene. A 50 mL round-bottom flask was charged with 3.04 g (8.80 mmol) of 4-(3,7-dimethyloctyloxy)-1-(trimethylsilylethynyl)benzene, 10 mL of CH₂Cl₂, and 10 mL of methanol. K₂CO₃ (0.24 g, 1.76 mmol) was added and the mixture stirred at room temperature overnight. The solvents were removed in vacuo, and the product was purified by column chromatography eluting with hexanes/ethyl acetate (99:1) to

yield an orange oil (2.15 g, 95%): $^1\text{H NMR}$ (400 MHz, CDCl_3) δ 0.88 (6H, d, $J = 8$ Hz), 0.94 (3H, d, $J = 8$ Hz), 1.62–1.85 (10H, overlapping multiplets), 3.0 (1H, s), 4.0 (2H, m), 6.84 (2H, d, $J = 8$ Hz), 7.43 (2H, d, $J = 12$ Hz); $^{13}\text{C NMR}$ (100 MHz, CDCl_3) δ 19.9, 22.8, 22.9, 24.9, 28.2, 30.0, 36.3, 37.5, 39.4, 66.5, 75.9, 83.7, 114.0, 114.6, 133.7, 159.7; HRMS (ESI) calcd for $\text{C}_{18}\text{H}_{27}\text{O}$ 259.2056 ($\text{M} + \text{H}$) $^+$, found 259.2060.

4-Dodecyl-1-ethynylbenzene. *Dodecylboronic Acid.* A dry, three-neck, 500 mL round-bottom flask was fitted with a reflux condenser, addition funnel, stir bar, and septum and placed under argon atmosphere. The flask was charged with 8.75 g (360 mmol) of magnesium turnings followed by a few crystals of iodine. Ether (300 mL) was added, the suspension was refluxed until a clear solution developed, and the flask was allowed to cool to room temperature. $\text{C}_{12}\text{H}_{25}\text{Br}$ (74.8 g, 300 mmol) was added dropwise via addition funnel to maintain a gentle reflux and then heated to reflux for 2 h. A separate dry, three-neck, 1 L round-bottom flask was equipped with an addition funnel and mechanical stirrer and charged with 72.7 g (750 mmol) of $\text{B}(\text{OMe})_3$ and 500 mL of diethyl ether. The flask was cooled to 0 °C in an ice–water bath and the fresh $\text{C}_{12}\text{H}_{25}\text{MgBr}$ solution added via addition funnel. The viscous mixture was allowed to warm to room temperature overnight, cooled back to 0 °C, and quenched with 1 N HCl. The layers were separated, the aqueous layer was extracted with diethyl ether (3 \times), and the combined organic layers were washed with water (2 \times) and brine (1 \times) and dried over MgSO_4 . The solution was filtered and the solvent removed in vacuo. The crude product was purified by recrystallization from hexanes to yield white needles (24.2 g, 38% yield): $^1\text{H NMR}$ (400 MHz, CDCl_3) δ 1.39 (3H, m), 1.26 (9H, overlapping multiplets), 0.88 (3H, t, $J = 8$ Hz); $^{13}\text{C NMR}$ (100 MHz, CDCl_3) δ 0.3, 14.4, 22.9, 24.6, 29.6, 29.7, 29.82, 29.86, 29.92, 32.2, 32.6.

4-Dodecyl-1-(trimethylsilyl)benzene. A dry two-neck, round-bottom flask was fitted with a reflux condenser and septum and placed under argon atmosphere. The flask was charged with 7.71 g (36.6 mmol) of dodecylboronic acid, 0.43 g (0.6 mmol) of $\text{Pd}(\text{dppf})\text{Cl}_2$, 12.8 g (60.0 mmol) of K_3PO_4 , and 7.08 g (30.0 mmol) of 4-bromo-1-(trimethylsilyl)benzene. The flask was then charged with 60 mL of dry/degassed toluene and the mixture heated to 100 °C for 36 h then allowed to cool to room temperature. The solids were filtered, the filter cake was washed with hexanes, and the filtrate was concentrated in vacuo. The crude product was filtered through a silica gel plug eluting with hexanes. The impurities were removed by careful vacuum distillation to yield a dark yellow oil (7.98 g, 83% yield): $^1\text{H NMR}$ (400 MHz, CDCl_3) δ 0.41 (9H, s), 1.04 (3H, t, $J = 8$ Hz), 1.45 (18H, overlapped multiplets), 1.77 (2H, m), 2.74 (2H, t, $J = 8$ Hz), 7.32 (2H, d, $J = 8$ Hz), 7.59 (2H, d, $J = 8$ Hz); $^{13}\text{C NMR}$ (100 MHz, CDCl_3) δ 0.8, 14.4, 23.0, 29.7, 29.76, 29.86, 29.93, 29.98, 30.0, 36.3, 128.1, 133.5, 137.2, 143.8.

4-Dodecyl-1-iodobenzene. A round-bottom flask was equipped with a stir bar, charged with 4.78 g (15.0 mmol) of 4-dodecyl-1-(trimethylsilyl)benzene and 15 mL of CH_2Cl_2 , and cooled to 0 °C in an ice water bath. A solution of 3.04 g (18.75 mmol) of ICl in 6 mL of CH_2Cl_2 was added dropwise and the solution allowed to warm to room temperature over 1 h. The reaction was diluted with CH_2Cl_2 and quenched with saturated NaHSO_3 . The layers were separated, the aqueous layer was extracted with CH_2Cl_2 (3 \times), and the combined organic layers were washed with water (1 \times) and brine (3 \times) and dried over MgSO_4 . The solution was filtered and the solvent removed in vacuo. The crude product was purified by recrystallization at –20 °C from ethanol to yield glistening white flakes (4.94 g, 88% yield): mp < 35 °C; $^1\text{H NMR}$ (400 MHz, CDCl_3) δ 0.88 (3H, t, $J = 8$ Hz), 1.28 (18H, overlapped multiplets), 1.57 (2H, m), 2.53 (2H, t, $J = 8$ Hz), 6.93 (2H, d, $J = 8$ Hz), 7.58 (2H, d, $J = 8$ Hz); $^{13}\text{C NMR}$ (100 MHz, CDCl_3) δ 14.4, 22.9, 29.4, 29.6, 29.7, 29.8, 29.9, 31.5, 32.2, 35.7, 90.7, 130.8, 137.4, 142.7.

4-Dodecyl-1-(trimethylsilylethynyl)benzene. A dry round-bottom flask was placed under argon atmosphere and charged with 1.87 g (5.0 mmol) of 4-dodecyl-1-bromobenzene, 0.0702 g (0.1 mmol) of $\text{Pd}(\text{PPh}_3)_2\text{Cl}_2$, and 0.0095 g (0.05 mmol) of CuI . Dry/degassed Et_3N (35 mL) was added and the flask cooled to 0 °C in an ice–water bath.

Trimethylsilylacetylene (0.58 g, 6.5 mmol) was added slowly dropwise syringe over 10 min and the mixture stirred for 2 h at 0 °C then 24 h at room temperature. The mixture was poured into saturated NH_4Cl and extracted with hexanes (4 \times). The combined organic extracts were washed with 1 N HCl (3 \times), water (1 \times), and brine (1 \times) and dried over MgSO_4 . The solution was filtered, and the solvents were removed in vacuo. The product was filtered through a silica gel plug eluting with hexanes to yield a pale yellow oil (1.48 g, 87% yield): $^1\text{H NMR}$ (400 MHz, CDCl_3) δ 0.26 (9H, s), 0.90 (3H, t, $J = 8$ Hz), 1.27 (18H, overlapped multiplets), 1.60 (2H, m), 2.60 (2H, t, $J = 8$ Hz), 7.11 (2H, d, $J = 8$ Hz), 7.39 (2H, d, $J = 8$ Hz); $^{13}\text{C NMR}$ (100 MHz, CDCl_3) δ 0.3, 14.4, 23.0, 29.4, 29.6, 29.7, 29.9, 29.9, 31.5, 32.2, 93.4, 105.6, 120.4, 128.5, 132.1, 143.8.

4-Dodecyl-1-ethynylbenzene. A small round-bottom flask was equipped with a stir bar and charged with 1.48 g (4.36 mmol) of 4-dodecyl-1-(trimethylsilylethynyl)benzene, 5 mL of CH_2Cl_2 , and 5 mL of methanol. K_2CO_3 (0.17 g, 0.87 mmol) was added and the mixture stirred at room temperature for 4 h then diluted with 10 mL of water and 15 mL of CH_2Cl_2 . The layers were separated, and the aqueous layer was extracted with CH_2Cl_2 (3 \times). The combined organic layers were washed with water (1 \times) and brine (2 \times) and dried over MgSO_4 . The solution was filtered, and the solvents were removed in vacuo. The crude product was filtered through a silica gel plug eluting with hexanes to yield a pale yellow oil (1.16 g, 98% yield): $^1\text{H NMR}$ (400 MHz, CDCl_3) δ 0.90 (3H, t, $J = 8$ Hz), 1.31 (18H, overlapped multiplets), 1.59 (2H, m), 2.60 (2H, t, $J = 8$ Hz), 3.04 (2H, s), 7.14 (2H, d, $J = 8$ Hz), 7.41 (2H, d, $J = 8$ Hz); $^{13}\text{C NMR}$ (100 MHz, CDCl_3) δ 14.4, 22.9, 29.5, 29.6, 29.7, 29.8, 29.9, 29.9, 31.5, 32.2, 36.1, 76.6, 84.1, 119.4, 128.6, 132.2, 144.2.

4,8-Bis(1-hexynyl)-2,6-dimethylbenzo[1,2-d-4,5-d']-bioxazole (11b). A dry pear-bottom flask was placed under argon atmosphere and charged 0.70 g (2.00 mmol) of **8b**, 0.0702 g (0.10 mmol) of $\text{Pd}(\text{PPh}_3)_2\text{Cl}_2$, 0.019 g (0.10 mmol) of CuI , and 0.026 g (0.10 mmol) of PPh_3 and dissolved in 60 mL of dry/degassed THF. This solution was added to a degassed solution of 0.49 g of 1-hexyne (6.00 mmol) and 2.02 g (20.0 mmol) of diisopropylamine in 5 mL of dry THF under argon atmosphere in a two-neck round-bottom flask equipped with a reflux condenser. The solution was refluxed for 24 h. The mixture was allowed to cool to room temperature, and the volatile components were removed in vacuo. The crude product was dissolved in hot hexanes and filtered, and the filtrate was concentrated in vacuo. Further purification by recrystallization from hexanes resulted in white needles (0.62 g, 88% yield): mp 168–170 °C; $^1\text{H NMR}$ (400 MHz, CDCl_3) δ 0.98 (6H, t, $J = 8$ Hz), 1.55 (4H, m), 1.69 (4H, m), 2.63 (4H, t, $J = 8$ Hz), 2.72 (6H, s); $^{13}\text{C NMR}$ (100 MHz, CDCl_3) δ 13.8, 15.0, 20.1, 23.3, 30.9, 70.7, 98.1, 101.7, 139.7, 148.8, 165.3; HRMS (ESI) calcd for $\text{C}_{22}\text{H}_{25}\text{N}_2\text{O}_2$ 349.1911 ($\text{M} + \text{H}$) $^+$, found 349.1913.

4,8-Bis(trimethylsilylethynyl)-2,6-dimethylbenzo[1,2-d-4,5-d']bioxazole (12b). A dry three-neck, round-bottom flask equipped with a reflux condenser and addition funnel was placed under argon atmosphere and charged with 3.74 g (10.0 mmol) of **8b**, 0.35 g (0.5 mmol) of $\text{PdCl}_2(\text{PPh}_3)_2$, 0.095 g (0.5 mmol) of CuI , 0.13 g (0.5 mmol) of PPh_3 , 10.1 g (100 mmol) of degassed diisopropylamine, and 150 mL of dry/degassed THF. A solution of 2.95 g (30.0 mmol) of trimethylsilylacetylene diluted in 12 mL of degassed THF was added dropwise at room temperature and the mixture heated to 50 °C overnight. The mixture was allowed to cool to room temperature, and the volatile components were removed in vacuo. The crude product was dissolved in hot hexanes and filtered, and the filtrate was concentrated in vacuo. The product was further purified by recrystallization from ethanol to yield white flakes (1.87 g, 49% yield): mp > 260 °C; $^1\text{H NMR}$ (400 MHz, CDCl_3) δ 0.63 (18H, s), 2.75 (6H, s); $^{13}\text{C NMR}$ (100 MHz, CDCl_3) δ 0.21, 15.2, 94.0, 98.3, 106.8, 140.0, 149.1, 165.9; HRMS (ESI) calcd for $\text{C}_{20}\text{H}_{25}\text{N}_2\text{O}_2\text{Si}_2$ 380.13762 ($\text{M} + \text{H}$) $^+$, found 380.13853.

4,8-Bis(phenylethynyl)-2,6-dimethylbenzo[1,2-d-4,5-d']-bioxazole (13b). Prepared similarly to **11b** from **8b** and phenylacetylene. Purified by recrystallization from chloroform/ethanol to yield small yellow needles (0.62 g, 78% yield): mp > 260 °C; $^1\text{H NMR}$ (400 MHz, CDCl_3) δ 2.78 (6H, s), 7.40 (6H, m), 7.22 (4H, m); ^{13}C

NMR (100 MHz, CDCl₃) δ 15.2, 79.5, 98.2, 100.1, 122.6, 128.5, 129.3, 132.3, 148.7, 165.9; HRMS (ESI) calcd for C₂₆H₁₇N₂O₂, 389.1285 (M + H)⁺, found 389.1287.

4,8-Bis(4-(3,7-dimethyloctyloxy)phenylethynyl)-2,6-dimethylbenzo[1,2-d-4,5-d']bisoxazole (14b). Prepared similarly to **11b** from **8b** and 1-(3,7-dimethyloctyloxy)-4-ethynylbenzene. The product was purified by recrystallization from ethanol to yield yellow needles (0.59 g, 84% yield): mp 163–165 °C; ¹H NMR (400 MHz, CDCl₃) δ 0.88 (12H, d, *J* = 8 Hz), 0.96 (6H, d, *J* = 8 Hz), 1.67–1.88 (10H, overlapping multiplets), 2.77 (6H, s), 4.05 (4H, m), 6.91 (4H, d, *J* = 8 Hz), 7.64 (4H, d, *J* = 8 Hz); ¹³C NMR (100 MHz, CDCl₃) δ 15.2, 19.9, 22.8, 24.9, 28.2, 30.1, 36.3, 37.5, 39.5, 66.6, 78.4, 98.2, 100.3, 114.5, 114.7, 133.9, 139.5, 148.6, 160.0, 165.6; HRMS (ESI) calcd for C₄₆H₅₇N₂O₄, 701.4313 (M + H)⁺, found 701.4315.

4,8-Bis(4-dodecylphenylethynyl)-2,6-dimethylbenzo[1,2-d-4,5-d']bisoxazole (15b). Prepared similarly to **11b** from **8b** and 4-dodecyl-1-ethynylbenzene. The product was purified by recrystallization from ethanol to yield small white needles (0.53 g, 73% yield): mp 194–197 °C; ¹H NMR (400 MHz, CDCl₃) δ 0.88 (6H, d, *J* = 8 Hz), 1.27–1.31 (36H, overlapped multiplets), 1.63 (4H, m), 2.64 (4H, t, *J* = 8 Hz), 2.75 (6H, s), 7.20 (4H, d, *J* = 8 Hz), 7.62 (4H, d, *J* = 8 Hz); ¹³C NMR (100 MHz, CDCl₃) 14.4, 15.1, 22.9, 29.5, 29.6, 29.7, 29.8, 29.86, 29.89, 31.4, 32.1, 36.2, 79.0, 98.2, 100.3, 119.8, 128.6, 132.2, 139.6, 144.5, 148.7, 165.7; HRMS (ESI) calcd for C₅₀H₆₅N₂O₂, 725.5041 (M + H)⁺, found 725.5031.

4,8-Dibromo-2,6-dimethylbenzo[1,2-d-4,5-d']bisoxazole Diethylphosphonate Ester (8f). A dry pressure flask was equipped with a stir bar, capped with a septum, and placed under argon atmosphere. The flask was charged with 2.68 g (6.46 mmol) of **8c** and 3.23 g (19.4 mmol) of triethyl phosphate, the flask sealed with a Teflon cap, and the mixture heated to 150 °C for 6 h. The mixture was allowed to cool to room temperature, the crude product dissolved in a minimal amount of CHCl₃, and the product precipitated into 5× the volume of heptanes. The precipitate was collected by filtration and washed with heptanes to yield a yellow-white powder (3.62 g, 91% yield): mp 163–165 °C; ¹H NMR (400 MHz, CDCl₃) δ 1.40 (12H, t, *J* = 8 Hz), 3.66 (4H, d, *J* = 28 Hz), 4.23 (8H, m); ¹³C NMR (100 MHz, CDCl₃) δ 16.5 (d, ³*J* = 5 Hz), 27.9 (d, ¹*J* = 138 Hz), 63.4 (d, ²*J* = 7 Hz), 92.0, 138.9, 147.2, 160.9 (d, ²*J* = 11 Hz); HRMS (EI) calcd for C₁₈H₂₀N₂O₈P₂Br₂, 615.93746 (M⁺), found 615.93965.

4,8-Dichloro-2,6-dimethylbenzo[1,2-d-4,5-d']bisoxazole Diethylphosphonate Ester (9f). Prepared similarly to **8f** from **9c** and triethyl phosphite to yield an off-white powder (4.79 g, 91% yield): mp 164–165 °C; ¹H NMR (400 MHz, CDCl₃) δ 1.38 (12H, t, *J* = 8 Hz), 3.67 (4H, d, *J* = 28 Hz), 4.25 (8H, m); ¹³C NMR (100 MHz, CDCl₃) δ 16.5 (d, ³*J* = 5 Hz), 29.2 (d, ¹*J* = 138 Hz), 63.4 (d, ²*J* = 7 Hz), 104.8, 137.7, 145.9, 161.3 (d, ²*J* = 11 Hz); HRMS (ESI) calcd for C₁₈H₂₅N₂O₈Cl₂P₂, 529.0458 (M + H)⁺, found 529.0460.

4,8-Bis(decynyl)-2,6-dimethylbenzo[1,2-d-4,5-d']bisoxazole Diethylphosphonate eEster (16f). A dry, two-neck round-bottom flask was equipped with a stir bar and reflux condenser and placed under argon atmosphere. Dry/degassed THF (140 mL, 9.11 g), diisopropylamine (90.0 mmol), and 1-decyne (3.73 g, 27.0 mmol) were added, and the mixture was degassed for 15 min. The flask was then charged with 5.56 g (9.00 mmol) of **8f**, 0.095 g (0.36 mmol) of PdCl₂(PPh₃)₂, 0.068 g (0.36 mmol) of PPh₃, and 0.25 g (0.36 mmol) of CuI. The solution was degassed for 10 min and heated to reflux for 24 h. The solution was allowed to cool to room temperature, and the volatile components were removed in vacuo. The crude product was filtered through a short silica plug eluting with Et₂O/CHCl₃ (4:1). The product was further purified by recrystallization from hexanes to yield a yellow solid (4.87 g, 74% yield): mp 119–120 °C; ¹H NMR (400 MHz, CDCl₃) δ 1.87 (6H, t, *J* = 8 Hz), 1.28–1.35 (16H, overlapping multiplets), 1.36 (12H, *J* = 8 Hz), 1.46 (4H, m), 1.69 (4H, quintet, *J* = 8 Hz), 2.58 (4H, t, *J* = 8 Hz), 3.64 (4H, d, *J* = 24 Hz), 4.22 (8H, m); ¹³C NMR (100 MHz, CDCl₃) δ 14.3, 16.5 (d, ³*J* = 6 Hz), 20.4, 22.9, 27.8 (d, ¹*J* = 137 Hz), 28.8, 29.3, 29.35, 29.39, 32.1, 63.3 (d, ³*J* = 6 Hz), 70.6, 98.9, 102.3, 140.0, 149.3, 160.4 (d, ²*J* = 25 Hz); HRMS (ESI) calcd for C₅₈H₈₃N₂O₈P₂, 997.5619 (M + H)⁺, found 997.5631.

4,8-Bis(4-dodecylphenylethynyl)-2,6-dimethylbenzo[1,2-d-4,5-d']bisoxazole Diethylphosphonate Ester (15f). Prepared similarly to **16f** from **8f** and 4-(dodecyl)-1-ethynylbenzene to yield a bright yellow powder (5.15 g, 65% yield): mp 110–111 °C; ¹H NMR (400 MHz, CDCl₃) δ 0.89 (6H, t, *J* = 8 Hz), 1.27–1.35 (36H, overlapping multiplets), 1.38 (12H, t, *J* = 8 Hz), 1.63 (4H, m), 2.64 (4H, t, *J* = 8 Hz), 3.67 (4H, d, *J* = 28 Hz), 4.25 (8H, m), 7.21 (4H, d, *J* = 8 Hz), 7.57 (4H, d, *J* = 8 Hz); ¹³C NMR (100 MHz, CDCl₃) δ 14.3, 16.6 (d, ³*J* = 6 Hz), 22.9, 27.86 (d, ¹*J* = 138 Hz), 27.9, 29.5, 29.6, 29.7, 29.8, 29.8, 29.9, 29.9, 31.4, 32.1, 63.4 (d, ²*J* = 6 Hz), 78.9, 99.0, 100.8, 119.8, 128.7, 132.1, 139.9, 144.7, 149.1, 160.6 (d, ²*J* = 9 Hz); HRMS (ESI) calcd for C₃₈H₅₉N₂O₈P₂, 733.3741 (M + H)⁺, found 733.3739.

General Polymerization Procedure (P1, P3, P4, and P5). A dry Schlenk flask was placed under argon atmosphere and charged with equimolar amounts of phosphonate ester **8f** (**P1**, **P4**), **9f** (**P5**), or **15f** (**P3**) and 2,5-didodecyloxyterephthaldehyde (**P1**, **P3**) or 3,4-didodecylthiophene dicarboxaldehyde (**P4**, **P5**) dissolved in dry THF to make a 0.06 M solution of phosphonate ester. The mixture was stirred at room temperature while adding 2.5 equiv of potassium *tert*-butoxide (1.0 M in THF) in one portion. The mixture was stirred at room temperature for 3 days, the reaction diluted 1.3 times with dry THF, and the reaction stirred for 2 additional days before the polymer was precipitated into 200 mL of methanol. The precipitated polymer was filtered into a cellulose extraction thimble, placed into a Soxhlet extractor and washed with methanol, hexane, and THF (**P1** and **P3**, and **P5**) or CHCl₃ (**P6**). Polymer was recovered from the THF or CHCl₃ extract by evaporation of the solvent.

Polymer P1: 0.45 g, 56% yield; ¹H NMR δ 0.88 (–CH₃, broad), 1.25–1.96 (–C₁₀H₂₅, broad), 4.13 (–OCH₂, broad), 6.9–7.25 (aryl-H and vinyl protons, broad); UV–vis (THF) λ_{max} = 476 nm; GPC *M_n* = 3300, *M_w* = 7900, PDI = 2.4; fluorescence (THF) λ_{em} = 524 nm (λ_{exc} = 476 nm).

Polymer P3: 0.33 g, 55% yield; ¹H NMR (400 MHz, CDCl₃) δ 0.89 (–CH₃, t), 1.25–1.20 (–C₁₁H₂₅, broad) 2.46 (aryl –CH₂, broad), 3.64 (OCH₂, broad), 6.93–7.00–7.25 (aryl, vinyl –CH, broad), 7.25–8.0 (aryl –CH, broad); UV–vis (THF) λ_{max} = 520 nm; GPC *M_n* = 5708, *M_w* = 14120, PDI = 2.5; fluorescence (THF) λ_{em} = 601 nm (λ_{exc} = 520 nm).

Polymer P4: 0.25 g, 61% yield; ¹H NMR (400 MHz, CDCl₃) δ 0.88 (–CH₃, t), 1.20–1.45 (–C₁₁H₂₅, broad), 2.77 (–CH₂, broad), 6.92–7.00 (vinyl –CH, broad), 8.02–8.04 (vinyl –CH, broad); UV–vis (THF) λ_{max} = 506 nm; GPC *M_n* = 4300, *M_w* = 6000, PDI = 1.4; fluorescence (THF) λ_{em} = 563 nm (λ_{exc} = 506 nm).

Polymer P5: 0.20 g, 55% yield; ¹H NMR (400 MHz, CDCl₃) δ 0.88 (–CH₃, t), 6.93–7.00 (–C₁₁H₂₅, broad), 2.78 (–CH₂, broad), 6.92–7.00 (vinyl –CH, broad), 7.98–8.04 (vinyl –CH, broad); UV–vis (THF) λ_{max} = 510 nm; GPC *M_n* = 3300, *M_w* = 7900, PDI = 2.4; fluorescence (THF) λ_{em} = 560 nm (λ_{exc} = 495 nm).

Polymer P2. A dry Schlenk flask was placed under argon atmosphere and charged with 0.36 g (0.50 mmol) of **16f**, 0.25 g (0.50 mmol) of 2,5-didodecyloxyterephthaldehyde, 0.11 g (1.25 mmol) of LiBr, and 9 mL of dry THF. The mixture was stirred at room temperature, 0.12 g (2.40 mmol) of Et₃N diluted in 1 mL of THF was added dropwise, the reaction was stirred for 3 days, and the polymer was precipitated into 150 mL of methanol. The precipitated polymer was filtered into a cellulose extraction thimble, placed in a Soxhlet extractor, and washed with methanol, hexane, and THF. The polymer was recovered from the THF extract by evaporation of the solvent (0.40 g, 87% yield): ¹H NMR (400 MHz, CDCl₃) δ 0.92, (–CH₃, broad), 1.35–1.64 (–C₁₁H₂₅, –C₆H₁₂, broad) 2.70 (propargyl –CH₂, broad), 3.25 (–OCH₂, broad), 6.93–7.00 (–C₁₁H₂₂, 7.04–7.25 (vinyl, aryl –CH, broad), 7.25–7.75 (aryl –CH, broad); UV–vis (THF) λ_{max} = 491 nm; GPC *M_n* = 22683, *M_w* = 113798, PDI = 5.0; fluorescence (THF) λ_{em} = 576 nm (λ_{exc} = 491 nm).

Computational Details. All of the calculations on the oligomers studied in this work were performed using the Gaussian 03W with the GaussView 4 GUI interface program package. All electronic ground states were optimized using density functional theory (DFT), B3LYP/6-31G*. Excited states were generated through time-dependent density functional theory (TD-DFT) applied to the optimized ground

state for each oligomer. The HOMO, LUMO, band gap, first 10 excited states, and UV-vis simulations were generated from these excited computations. Approximations of the molecular orbital contributions for each excited state were obtained using the GaussSum 2.2 freeware package. Finally, electrostatic potential maps were created using a coarse setting and an isovalue of 0.03.

■ ASSOCIATED CONTENT

● Supporting Information

Experimental procedures, ^1H and ^{13}C NMR spectra for new compounds, and tables of the calculated atom coordinates and absolute energies. This material is available free of charge via the Internet at <http://pubs.acs.org>.

■ AUTHOR INFORMATION

Corresponding Author

*E-mail: malikaj@iastate.edu.

■ ACKNOWLEDGMENTS

We acknowledge the donors of the American Chemical Society Petroleum Research Fund for support of this research. We also thank the 3M Foundation and the National Science Foundation (DMR-0846607) and Teragrid (TG-CHE100148) for partial support of this work. We thank Dr. Kamel Harrata and the Mass Spectroscopy Laboratory of Iowa State University (ISU) for analysis of our compounds and Dr. Arkady Ellern for X-ray crystallographic analysis. We thank Atta Gueye, Dr. Elena Sheina, and Dr. Christopher Brown of Plextronics for providing UPS measurements. We thank Scott Meester for the synthesis of 4-(3,7-dimethyloctyloxy)-1-bromobenzene and Andrew Makowski for the synthesis of 2,5-didodecyloxyterephthaldehyde. We also thank Dr. Toby Nelson and Dr. David Yaron (Carnegie Mellon University) for helpful discussions of this research.

■ REFERENCES

- (1) Horowitz, G. *Adv. Mater.* **1998**, *10* (5), 365–377.
- (2) Mas-Torrent, M.; Rovira, C. *Chem. Soc. Rev.* **2008**, *37* (4), 827–838.
- (3) Newman, C. R.; Frisbie, C. D.; daSilva Filho, D. A.; Bredas, J. L.; Ewbank, P. C.; Mann, K. R. *Chem. Mater.* **2004**, *16* (23), 4436–4451.
- (4) Murphy, A. R.; Frechet, J. M. J. *Chem. Rev.* **2007**, *107* (4), 1066–1096.
- (5) Dimitrakopoulos, C. D.; Malenfant, P. R. L. *Adv. Mater.* **2002**, *14* (2), 99–117.
- (6) Tang, C. W.; VanSlyke, S. A. *Appl. Phys. Lett.* **1987**, *51* (12), 913–915.
- (7) Veinot, J. G. C.; Marks, T. J. *Acc. Chem. Res.* **2005**, *38* (8), 632–643.
- (8) Friend, R. H.; Gymer, R. W.; Holmes, A. B.; Burroughes, J. H.; Marks, R. N.; Taliani, C.; Bradley, D. D. C.; Dos Santos, D. A.; Bredas, J. L.; Logdlund, M.; Salaneck, W. R. *Nature* **1999**, *397* (6715), 121–128.
- (9) Alam, M. M.; Jenekhe, S. A. *Chem. Mater.* **2004**, *16* (23), 4647–4656.
- (10) Coakley, K. M.; McGehee, M. D. *Chem. Mater.* **2004**, *16* (23), 4533–4542.
- (11) Scharber, M. C.; Muehlbacher, D.; Koppe, M.; Denk, P.; Waldauf, C.; Heeger, A. J.; Brabec, C. J. *Adv. Mater.* **2006**, *18* (6), 789–794.
- (12) Tang, C. W. *Appl. Phys. Lett.* **1986**, *48* (2), 183–185.
- (13) Osaheni, J. A.; Jenekhe, S. A. *J. Am. Chem. Soc.* **1995**, *117* (28), 7389–7398.
- (14) Havinga, E. E.; ten Hoeve, W.; Wynberg, H. *Synth. Met.* **1993**, *55* (1), 299–306.
- (15) van Mullekom, H. A. M.; Vekemans, J. A. J. M.; Havinga, E. E.; Meijer, E. W. *Mater. Sci. Eng., R* **2001**, *32* (1), 1–40.
- (16) Zhou, H.; Yang, L.; Stoneking, S.; You, W. *ACS Appl. Mater. Interfaces* **2010**, *2* (5), 1377–1383.
- (17) Roncali, J. *Chem. Rev.* **1997**, *97* (1), 173–205.
- (18) Zhu, Y.; Champion, R. D.; Jenekhe, S. A. *Macromolecules* **2006**, *39* (25), 8712–8719.
- (19) So, Y.-H.; Martin, S. J.; Bell, B.; Pfeiffer, C. D.; Van Effen, R. M.; Romain, B. L.; Lefkowitz, S. M. *Macromolecules* **2003**, *36* (13), 4699–4708.
- (20) Klare, J. E.; Tulevski, G. S.; Sugo, K.; de Picciotto, A.; White, K. A.; Nuckolls, C. *J. Am. Chem. Soc.* **2003**, *125* (20), 6030–6031.
- (21) Osowska, K.; Miljanic, O. S. *Chem. Commun.* **2010**, *46* (24), 4276–4278.
- (22) Klare, J. E.; Tulevski, G. S.; Nuckolls, C. *Langmuir* **2004**, *20* (23), 10068–10072.
- (23) Mike, J. F.; Makowski, A. J.; Mauldin, T. C.; Jeffries-El, M. J. *Poly. Sci. A* **2010**, *48* (6), 1456–1460.
- (24) Mike, J. F.; Nalwa, K.; Makowski, A. J.; Putnam, D.; Tomlinson, A. L.; Chaudhary, S.; Jeffries-El, M. *Phys. Chem. Chem. Phys.* **2011**, *13* (4), 1338–1344.
- (25) Patil, A. V.; Park, H.; Lee, E. W.; Lee, S.-H. *Synth. Met.* **2010**, *160* (19–20), 2128–2134.
- (26) Anslyn, E. V.; Dougherty, D. A. *Modern Physical Organic Chemistry*; University Sciences: Sausalito, CA, 2004.
- (27) Anthony, J. E.; Brooks, J. S.; Eaton, D. L.; Parkin, S. R. *J. Am. Chem. Soc.* **2001**, *123* (38), 9482–9483.
- (28) Anthony, J. E.; Eaton, D. L.; Parkin, S. R. *Org. Lett.* **2001**, *4* (1), 15–18.
- (29) Anthony, J. E.; Facchetti, A.; Heeney, M.; Marder, S. R.; Zhan, X. *Adv. Mater.* **2010**, *22* (34), 3876–3892.
- (30) Swartz, C. R.; Parkin, S. R.; Bullock, J. E.; Anthony, J. E.; Mayer, A. C.; Malliaras, G. G. *Org. Lett.* **2005**, *7*, 3163–6.
- (31) Miao, S.; Smith, M. D.; Bunz, U. H. F. *Org. Lett.* **2006**, *8* (4), 757–760.
- (32) Appleton, A. L.; Miao, S.; Brombosz, S. M.; Berger, N. J.; Barlow, S.; Marder, S. R.; Lawrence, B. M.; Hardcastle, K. I.; Bunz, U. H. F. *Org. Lett.* **2009**, *11* (22), 5222–5225.
- (33) Hilger, A.; Gisselbrecht, J.-P.; Tykewinski, R. R.; Boudon, C.; Schreiber, M.; Martin, R. E.; Luethi, H. P.; Gross, M.; Diederich, F. *J. Am. Chem. Soc.* **1997**, *119* (9), 2069–2078.
- (34) Rose, B. D.; Chase, D. T.; Weber, C. D.; Zakharov, L. N.; Loneragan, M. C.; Haley, M. M. *Org. Lett.* **2011**, *13* (8), 2106–2109.
- (35) Mike, J. F.; Makowski, A. J.; Jeffries-EL, M. *Org. Lett.* **2008**, *10* (21), 4915–4918.
- (36) Liao, J.; Wang, Q. *Macromolecules* **2004**, *37* (18), 7061–7063.
- (37) Destri, S.; Pasini, M.; Pelizzi, C.; Porzio, W.; Predieri, G.; Vignali, C. *Macromolecules* **1999**, *32* (2), 353–360.
- (38) Rathke, M. W.; Nowak, M. *J. Org. Chem.* **1985**, *50* (15), 2624–2626.
- (39) Salaneck, W. R. *J. Electron Spectrosc. Relat. Phenom.* **2009**, *174* (1–3), 3–9.
- (40) Miyamae, T.; Yoshimura, D.; Ishii, H.; Ouchi, Y.; Miyazaki, T.; Koike, T.; Yamamoto, T.; Muramatsu, Y.; Etori, H.; Maruyama, T.; Seki, K. *Synth. Met.* **1997**, *84* (1–3), 939–940.
- (41) Lois, S.; Florès, J.-C.; Lère-Porte, J.-P.; Serein-Spirau, F.; Moreau, J. E.; Miquieu, K.; Sotiropoulos, J.-M.; Baylère, P.; Tillard, M.; Belin, C. *Eur. J. Org. Chem.* **2007**, *2007* (24), 4019–4031.
- (42) Becke, A. D. *J. Chem. Phys.* **1993**, *98* (7), 5648–5652.
- (43) Blouin, N.; Michaud, A.; Gendron, D.; Wakim, S.; Blair, E.; Neagu-Plesu, R.; Belletete, M.; Durocher, G.; Tao, Y.; Leclerc, M. *J. Am. Chem. Soc.* **2008**, *130* (2), 732–742.
- (44) Belletete, M.; Blouin, N.; Boudreault, P.-L. T.; Leclerc, M.; Durocher, G. *J. Phys. Chem. A* **2006**, *110* (51), 13696–13704.
- (45) Belletete, M.; Durocher, G.; Hamel, S.; Cote, M.; Wakim, S.; Leclerc, M. *J. Chem. Phys.* **2005**, *122* (10), 104303–9.
- (46) Zade, S. S.; Bendikov, M. *Org. Lett.* **2006**, *8* (23), 5243–5246.
- (47) Cai, Z.-L.; Sendt, K.; Reimers, J. R. *J. Chem. Phys.* **2002**, *117* (12), 5543–5549.

- (48) Dreuw, A.; Head-Gordon, M. *J. Am. Chem. Soc.* **2004**, *126* (12), 4007–4016.
- (49) Reimers, J. R.; Cai, Z. L.; Bilić, A.; Hush, N. S. *Ann. N.Y. Acad. Sci.* **2003**, *1006* (1), 235–251.
- (50) Kaur, I.; Jia, W.; Kopreski, R. P.; Selvarasah, S.; Dokmeci, M. R.; Pramanik, C.; McGruer, N. E.; Miller, G. P. *J. Am. Chem. Soc.* **2008**, *130* (48), 16274–16286.
- (51) Yasuda, T.; Imase, T.; Nakamura, Y.; Yamamoto, T. *Macromolecules* **2005**, *38* (11), 4687–4697.
- (52) Levitus, M.; Schmieder, K.; Ricks, H.; Shimizu, K. D.; Bunz, U. H. F.; Garcia-Garibay, M. A. *J. Am. Chem. Soc.* **2001**, *123* (18), 4259–4265.
- (53) O'Boyle, N. M.; Tenderholt, A. L.; Langner, K. M. *J. Comput. Chem.* **2008**, *29* (5), 839–845.
- (54) Marsden, J. A.; Miller, J. J.; Shirtcliff, L. D.; Haley, M. M. *J. Am. Chem. Soc.* **2005**, *127* (8), 2464–2476.
- (55) Sista, P.; Nguyen, H.; Murphy, J. W.; Hao, J.; Dei, D. K.; Palaniappan, K.; Servello, J.; Kularatne, R. S.; Gnade, B. E.; Xue, B.; Dastoor, P. C.; Biewer, M. C.; Stefan, M. C. *Macromolecules* **2010**, *43* (19), 8063–8070.
- (56) Hundt, N.; Palaniappan, K.; Servello, J.; Dei, D. K.; Stefan, M. C.; Biewer, M. C. *Org. Lett.* **2009**, *11* (19), 4422–4425.
- (57) Zuccherro, A. J.; McGrier, P. L.; Bunz, U. H. F. *Acc. Chem. Res.* **2009**, *43* (3), 397–408.
- (58) Gierschner, J.; Cornil, J.; Egelhaaf, H.-J. *Adv. Mater.* **2007**, *19* (2), 173–191.
- (59) Milian Medina, B.; VanVooren, A.; Brocorens, P.; Gierschner, J.; Shkunov, M.; Heeney, M.; McCulloch, I.; Lazzaroni, R.; Cornil, J. *Chem. Mater.* **2007**, *19* (20), 4949–4956.
- (60) Mylari, B. L.; Scott, P. J.; Zembrowski, W. J. *Synth. Commun.* **1989**, *19* (16), 2921–2924.
- (61) Jones, R. G. *J. Am. Chem. Soc.* **1951**, *73*, 5168–5169.
- (62) Hegedus, L. S.; Odle, R. R.; Winton, P. M.; Weider, P. R. *J. Org. Chem.* **1982**, *47* (13), 2607–13.
- (63) Mike, J. F.; Inteman, J. J.; Ellern, A.; Jeffries-El, M. *J. Org. Chem.* **2010**, *75* (2), 495–497.